A Fast PEEC Technique for Full-Wave Parameters Extraction of Distributed Elements

Swee Ann Teo, Ban Leong Ooi, Siou Teck Chew, and Mook Seng Leong

***Abstract*—In this paper, a full wave partial element equivalent circuit (PEEC) technique using exact Green's function is introduced for the parameter extraction of a passive device in a homogeneous media over a wide frequency range from dc to a frequency of interest. This technique makes use of some analytical techniques and cartesian multipole expansion to derive simple closed form expressions for each individual element of the coupling matrices that commonly arise in integral equation algorithms, in terms of the wave number alone. Hence, these matrices can be reused each time a new frequency is selected. As simple closed form expressions are used, very fast computation is possible.**

***Index Terms*—Parameter extraction, PEEC.**

I. Introduction

THE problem of parameter extraction of passive microwave devices has received much attention as they are an indispensable part of circuit design. Recently, with the development of new processes such as low temperature cofired ceramics (LTCC), it has been of interest to develop a fast method for the characterization of passive devices embedded in a homogeneous media [1], [4]–[8].

In this paper, we have chosen to use the partial element equivalent circuit (PEEC) technique. This method is well suited for parameter extraction as it converts the device into an equivalent circuit model that can be simulated using a SPICE program.

In contrast to Garret's work [2], [3] we have taken a more general approach of using the exact Green's function instead, and a high order approximation later in the calculation of the coupling terms. By using analytical methods and cartesian multipole expansion, simple closed form expressions have been obtained for all the coupling terms with minimal error in terms of the wave number. Hence, having tabled a matrix of such expressions, it can be re-used at every different frequency.

II. Theory

In LTCC, where the metal strips are very thin, and thus it is convenient to use surface basis functions instead of volume basis functions.

The following parameters are obtained:

$$R_{m,n} = \int \sigma_s^{-1} \mathbf{J}_m(\mathbf{r}) \cdot \mathbf{J}_n(\mathbf{r}) \mathrm{d}s \tag{1}$$

$$L_{m,n} = \frac{\mu}{4\pi} \iint \psi(\mathbf{r}, \mathbf{r}') \mathbf{J}_m(\mathbf{r}) \cdot \mathbf{J}_n(\mathbf{r}') \mathrm{d}s \, \mathrm{d}s' \tag{2}$$

$$P_{m,n} = \frac{1}{4\pi\varepsilon} \iint \psi(\mathbf{r}, \mathbf{r}') \rho_m(\mathbf{r}) \rho_n(\mathbf{r}') \mathrm{d}s \, \mathrm{d}s' \tag{3}$$

where σ_s is the surface conductivity, and R, L, and P are analogous to resistance, inductance and the reciprocal of capacitance, respectively.

The computation of these integrals, especially (2) and (3), are very time consuming. In this paper, we reduce the computational requirement of evaluating such integrals by using a two-step method. Analytical techniques and cartesian multipole expansion are used to derive closed form series expressions for these integrals. These series expressions are subsequently used to derive simple closed form expressions for each element of the matrix in terms of the wave number alone. These expressions usually consist of no more than an exponential term, multiplied by a polynomial.

Therefore, instead of tabling a matrix at a certain frequency directly, we table the coupling matrices that are made up of these expressions. Due to the simplicity of expressions within the matrices, actual tabling of the various matrices at different frequencies becomes very efficient.

A. Self-Patch, $m = n$

In this section, we first approximate the free space Green's function using the following Laurent series of six terms:

$$\psi(\mathbf{r}, \mathbf{r}') \cong k \left[\frac{1}{R} - j - \frac{R}{2} + \frac{jR^2}{6} + \frac{R^3}{24} - \frac{jR^4}{120} \right] \tag{4}$$

where $R = k|\mathbf{r} - \mathbf{r}'|$. This approximate Green's function has an error of less than 0.6% for $R < 0.4\pi$. Thus, for this Green's function to cover a total width of 0.4λ, the maximum size of the basis function should be 0.2λ or less. Under such conditions, the self coupling term calculated using this approximation will have an error that is always less than 0.6%. As the size of the basis function should be about $\lambda/20$, the above approximation is sufficiently accurate for our analysis.

To proceed, we shall consider the integral in (3). Through a simple substitution, (3) shall be rewritten as

$$P_{0,0} = \frac{1}{4\pi\varepsilon} \int \psi(r'') \left[\int \rho_0(\mathbf{r}) \rho_0(\mathbf{r} - \mathbf{r}'') \mathrm{d}s \right] \mathrm{d}s'' \tag{5}$$

where $\mathbf{r}'' = \mathbf{r} - \mathbf{r}'$ and $r'' = |\mathbf{r}''|$. In order to obtain the value of the integral, we need to make use of the fact that the integrals of the following form:

$$\int_0^b \int_0^a \left(x^2 + y^2\right)^{n/2} f(x) g(y) \mathrm{d}x \, \mathrm{d}y \tag{6}$$

Manuscript received March 1, 2000; revised March 15, 2001. The review of this letter was arranged by Associate Editor R. Vahldieck.

The authors are with the Department of Electrical and Computing Engineering, National University of Singapore, Singapore 119260 (e-mail: eleooibl@nus.edu.sg).

Publisher Item Identifier S 1531-1309(01)04005-3.

have closed-form solutions for $n = -1, 0, 1, 2, \ldots$ when $f(x)$ and $g(y)$ are simple polynomials of x and y, respectively

$$\rho_0(x,y) = \begin{cases} \frac{1}{ab}, & |x| < \frac{a}{s} \text{ and } |y| < \frac{b}{2} \\ 0, & \text{otherwise.} \end{cases} \tag{7}$$

For instance, for $n = -1$, the following integral can be expressed as:

$$\begin{aligned} &\int_0^b \int_0^a (x^2+y^2)^{1/2} \frac{(a-x)(b-y)}{a^2b^2} \mathrm{d}x\,\mathrm{d}y \\ &\quad = \frac{1}{6a^2b^2}\Bigg[3ab^2 + 3b^3 - 2ab\sqrt{a^2+b^2} - 3b^2\sqrt{a^2+b^2} \\ &\qquad + a^2(a-3b)\log a + b^2(-6a+b)\log b \\ &\qquad + 6ab^2 \log\left(a + \sqrt{a^2+b^2}\right) \\ &\qquad - b^3 \log\left(a + \sqrt{a^2+b^2}\right) \\ &\qquad - a^3 \log\left(b + \sqrt{a^2+b^2}\right) \\ &\qquad + 3a^2 b \log\left(b + \sqrt{a^2+b^2}\right)\Bigg]. \end{aligned} \tag{8}$$

With these closed-form expressions, there is no need to perform any numerical integration in the algorithm, so long the basis functions are planar and can be expressed in terms of piecewise polynomial functions, such as rooftop and pulse basis functions. We notice that by using expression (4) with the computed results of (6) which are obtained using closed form solutions, simple expressions for the $P_{m,m}$ in terms of k can be derived. This expression was found to have negligible error compared to numerical integration for $R < 0.2\lambda$, where $R = \max(a,b)$.

In addition, the storage and computational speed have improved significantly.

B. Mutual Coupling, $m \neq n$

When the elements are not overlapping and far from one another, Taylor series expansion can be used to derive similar closed form expressions in terms of the wave number, i.e.

$$\begin{aligned} \psi(\mathbf{r}'') =& \psi_0\big(1 + \psi_{10}\delta x'' + \psi_{01}\delta y'' + \psi_{11}\delta x''\delta y'' \\ &+ \psi_{20}\delta x''^2 + \psi_{02}\delta y''^2 + \cdots\big) \end{aligned} \tag{9}$$

where ψ_0 is the free space Green function, and

$$\psi_{mn} = \frac{1}{m!n!}\frac{1}{\psi_0}\frac{\partial^m}{\partial x^m}\frac{\partial^n}{\partial y^n}\psi(\mathbf{r}'')\bigg|_{\mathbf{r}''=\mathbf{r}_0}. \tag{10}$$

Therefore, for the following integral:

$$W = \iint \psi(r'')X_1(x')X_1(y')X_2(x)Y_2(y)\mathrm{d}s'\mathrm{d}s$$

the expansion in (9) results in the following:

$$\begin{aligned} W =& \psi_0\big[X_2^0X_1^0Y_2^0Y_1^0 + \psi_{10}\big(X_2^1X_1^0 - X_2^0X_1^1\big)Y_2^0Y_1^0 \\ &+ \psi_{01}X_2^0X_1^0\big(Y_2^1Y_1^0 - Y_2^0Y_1^1\big) \\ &+ \psi_{11}\big(X_2^1X_1^0 - X_2^0X_1^1\big)\big(Y_2^1Y_1^0 - Y_2^0Y_1^1\big) + \cdots\big] \end{aligned} \tag{11}$$

where

$$X_n^m = \int X_n(x)x^m\mathrm{d}x \tag{12}$$

$$Y_n^m = \int Y_n(y)y^m\mathrm{d}y \tag{13}$$

are the mth moments of the X_i and Y_i functions, respectively. Using the odd and even function properties, further simplifications are possible. It is found in general that if the expansion is carried out to calculate the coupling between elements that are not overlapping, the degree for expansion serves as a very good approximation. The error increases when r_0 is smaller than the expansion radius. The expansion radius is defined as the largest value of δx or δy, used in the expansion.

C. Near Field Region Coupling

In the intermediate region, where the configuration falls into both of the near and far field regions as was in Sections II-A and II-B, closed-form solutions can be obtained by subdividing the basis functions into smaller parts and combining both expansions.

After the basis functions are divided into parts, the relevant expansions should be used. The coupling of overlapping and neighboring basis functions are to be calculated using the Laurent series expansion, and those that are further away are to be calculated using the cartesian expansion. The subdivision can be easily implemented using a recursive algorithm.

D. Modeling an Inductor

As an application of the technique, we shall model a 3–D helical two–turn inductor (See Fig. 3). To simplify the analysis, the component is assumed to be made up of flat narrow strips of a conducting material with some vertical vias. As such there is no transverse current component. This will allow us to build a simple circuit representation of the device.

The node voltage v_n, and node current, i_n, assume the form as

$$\mathbf{v} = (v_N, v_{N-1}, \ldots, v_1)^{\mathrm{T}} \tag{14}$$

$$\mathbf{i} = (i_{N-1}, i_{N-2}, \ldots, i_1)^{\mathrm{T}} \tag{15}$$

where $n = 1, 2, \ldots N$. Using voltage excitation, we let the two end nodes be connected to two voltage sources. Hence we obtain

$$\mathbf{v} = [T_1]\mathrm{v}_s + [T_2]\mathrm{v}_i \tag{16}$$

where

$$\mathbf{v_s} = (v_{N-1}, v_{N-2}, \ldots, v_2)^{\mathrm{T}} \tag{17}$$

$$\mathbf{v_i} = (v_N, v_1)^{\mathrm{T}} \tag{18}$$

and $[T_1]$ and $[T_2]$ are the relevant matrices to effect the transformation. The voltages and the currents are related to each other via the following relationships:

$$v_{n+1} - v_n = \sum_p (R_{p,n} + j\omega p_{p,n})i_p \tag{19}$$

$$v_{n+1} = \frac{1}{j\omega p}\sum_p p_{p,n}(i_{p+1} + i_p). \tag{20}$$

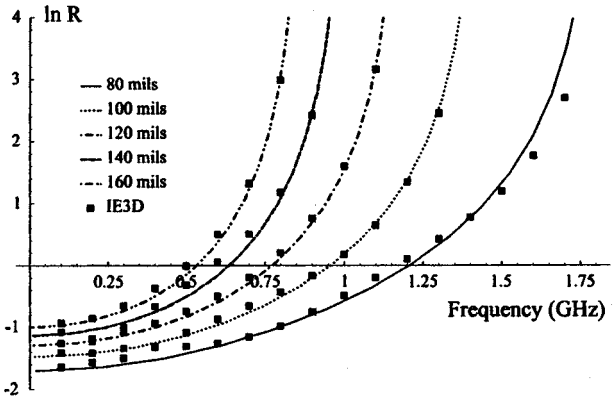

Fig. 1. $10\log_{10}$ of resistive losses of test circuit for different values of W calculated using proposed algorithm, compared with results obtained using IE3D.

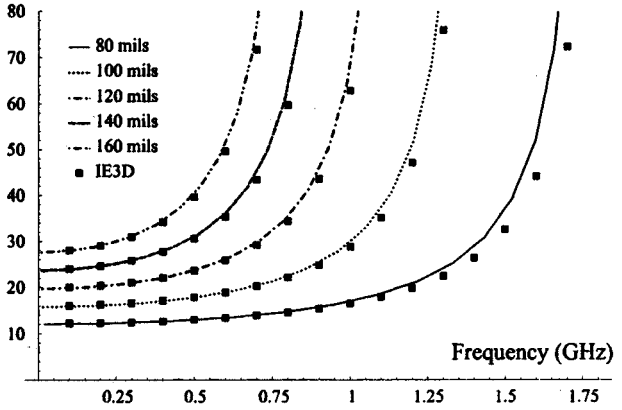

Fig. 2. Inductance of test circuit for different values of W calculated using proposed algorithm, compared with results obtained using IE3D.

Therefore, by making use of the above relationships, one can derive the current distribution on the wire and obtain the input impedance of the system. It is also possible to use these equations to obtain the Z-matrix of the two-port system.

E. Results for a 3-D Helical Inductor

The Inductor line width is set at 10 mils, and the substrate thickness is 7.5 mils for cases. The conductivity of the conductor used is 4.9×10^7 S/m and the via to ground passes through three layers. Using the above formulation for different values of W, the results are as shown in Figs. 1–3.

This method was found to be stable and accurate in its prediction of self resonant frequency (SRF), losses, and inductance.

Comparing with numerical integration, the use of the cartesian expansion accelerated the algorithm by an order of magnitude. Further increase in speed was achieved by using the technique to derive simple closed form expressions to represent the

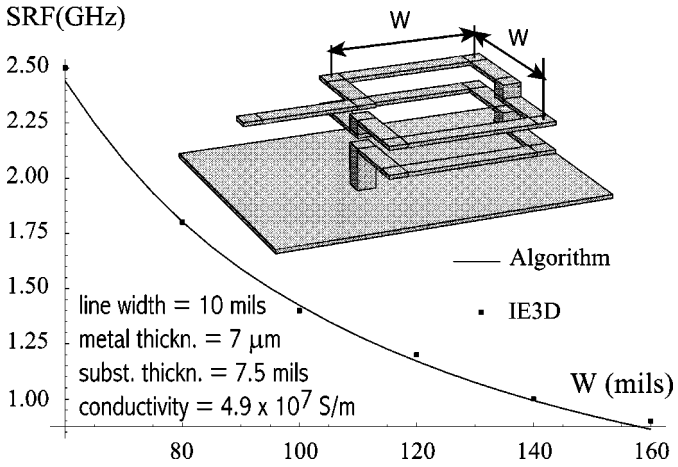

Fig. 3. Self-resonant frequency of test circuit for different values of W calculated using proposed algorithm, compared with results obtained using IE3D.

terms in the various matrices, so that extremely fast tabling of these matrices are possible at each different frequency point.

III. Conclusion

It was found that the use of cartesian expansion has allowed us to develop simple closed-form solutions for the coupling between the basis functions. These closed form solutions can be stored and used for each different frequency, thereby increasing the speed of tabling the coupling matrices.

The overhead of deriving such closed form expressions to be tabled into matrices via the above described techniques has also been found to be low. This method is particularly suitable for characterizing passive components, where simulation over large frequency range is required.

References

[1] U. Geigenmuller and N. P. van der Meijs, "Cartesian multipole based numerical integration for 3-D capacitance extraction," in *Proc. Eur. Design Test Conf.*, 1997, pp. 256–259.

[2] J. Garrett *et al.*, "Recent improvements in PEEC modeling accuracy," in *Proc. IEEE Int. Symp. Electromagnetic Compatibility 1997*, Aug. 1997, pp. 347–352.

[3] ——, "Stability improvements of integral equation models," in *Proc. IEEE Antennas Propagat. Soc. Int. Symp.*, vol. 3, 1997, pp. 1810–1813.

[4] J. Zhao *et al.*, "Modeling and design considerations for embedded inductors in MCM-D," in *Proc. Int. Conf. Multichip Modules*, Apr. 1997, pp. 334–339.

[5] A. Sutono *et al.*, "Development of three dimensional ceramic-based MCM inductors for hybrid RF/microwave applications," in *Proc. Radio Freq. Integr. Circuits (RFIC) Symp.*, 1999, pp. 175–178.

[6] K. Delanay *et al.*, "Charaterization of the electrical performance of buried capacitors and resistors in low temperature co-fired (LTCC) ceramic," in *Proc. IEEE Electron. Comp. Technol. Conf.*, 1998, pp. 900–908.

[7] M. Kamon *et al.*, "FASTHENRY: A multipole-accelerated 3-D inductance extraction program," *IEEE Trans. Microwave Theory Tech.*, vol. 42, pp. 1750–1758, Sept. 1994.

[8] ——, "Efficient techniques for inductance extraction of complex 3-D geometries," in *Proc. 1992 IEEE/ACM Int. Conf.*, Nov. 1992, pp. 438–442.